Journal of Statistical Physics, Vol. 76, Nos. 5/6, 1994

Exact Scaling Behavior of Partially Convex Vesicles

?. Brak,[1] A. L. Owczarek,[1] and T. Prellberg[1]

Received February 3, 1994

We solve analytically for the perimeter–area generating functions for two models of vesicles. While from the solution of the first model, staircase polygons, one can easily extract the asymptotic scaling behavior, the exact solution of the second, column-convex polygons, is difficult to analyze. This leads us to apply a recently developed method for deriving the scaling behavior indirectly, utilizing a set of nonlinear differential equations. One result of this work is a nontrivial confirmation of the scaling/universality hypothesis.

KEY WORDS: Exact solution; scaling; vesicles; column-convex polygons; staircase polygons.

1. INTRODUCTION

Whenever a new model is introduced which undergoes a continuous phase transition it is always desirable to calculate the critical exponents exactly. In the past few year there have been several exact solutions given for partially directed models of vesicles,[1–4] walks,[5,6] and interfaces[7,8] on the square lattice. The solutions for the full area–perimeter generating functions for the vesicle models have been written down in terms of q-hypergeometric functions. While these works provide the "exact" solution, the asymptotics of these functions have been elusive and hence the critical behavior has not been extracted. Work on partially directed interacting walks[6] has provided two distinct approaches to this problem. The first is to consider the partially directed object in the limit when one lattice direction has been made continuous. This has proved fruitful[6,9] since the generating functions can usually now be written in terms of Bessel functions. Furthermore, the "semicontinuous" model's solution can be obtained

[1] Department of Mathematics, University of Melbourne, Parkville, Victoria 3052, Australia. e-mail: brak,aleks,prel@mundoe.maths.mu.oz.au.

0022-4715/94/0900-1101$07.00/0

by taking the continuum limit of the discrete model's solution. The second approach, through a formal perturbation expansion, is able to give several critical exponents. In a new development[10] the continuum limit has been applied to a different representation of the generating function to obtain nonlinear differential equations from which the scaling behavior of the generating function can be derived.

In this paper we shall demonstrate the power of these three methods by examining the scaling behavior of two vesicle models whose scaling behavior has not been previously discussed. These models are staircase polygons and column-convex polygons. Both these models have been solved for their generating functions. We shall first exactly solve the semi-continuous partners of these models. For staircase polygons, where the solution is in terms of Bessel functions (${}_0F_1$ hypergeometric functions) again, the scaling behavior can be extracted with ease. In the second, the solution is in terms of functions proportional to ${}_0F_3$ hypergeometric functions. Moreover, the solution is no longer a simple ratio of hypergeometric functions, but rather has such a complicated structure that further analysis is prohibitively complex. The continuum limit method[10] is then applied to both lattice models. All the results of this method agree with those found from the semicontinuous solution. Further, the result gives us the full scaling solution of the column-convex polygon model. The method of solution, when applied to column-convex polygons, is complex and requires the use of computer algebraic manipulation.

The two models, staircase and column-convex polygons, are believed to be in the same universality class. Our work not only confirms that the critical exponents are identical for these models, but also that the scaling functions are the same (though with different, nonuniversal, amplitudes). This provides an example of the scaling/universality hypothesis being upheld in a situation where exact solutions are available. Another bonus of our work is that the solution of the scaling behavior of column-convex polygons sheds light on the mathematical approximations made in the study[11-13] of the bubble model of low-temperature correlations in Ising systems (previous work had "approximated" column-convex polygons by bar-graph polygons).

Column-convex polygons are self-avoiding polygons on the square lattice with the additional constraint that any vertical line on the dual lattice only intersects two edges of the polygon (and hence is partially convex). A typical column-convex polygon is shown in Fig. 1. This model was introduced by Temperley,[14] who called it model Q and it has also been referred to as row-convex polygons by others.[1,2] Another, simpler model of vesicles is staircase polygons. These are self-avoiding polygons on the square lattice with the additional constraint that the upper and lower

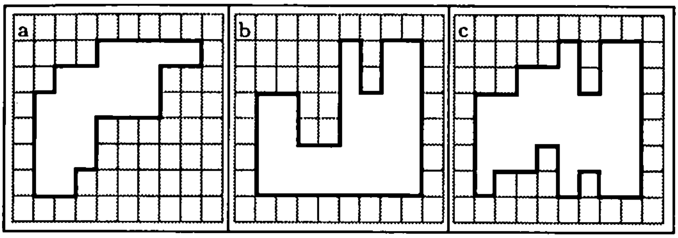

Fig. 1. Typical configurations for (a) staircase polygons, (b) bar-graph polygons, and (c) column-convex polygons.

bounding walks can only step in a north or east direction. The upper and lower walks start at the bottom lefmost corner and end at the upper rightmost corner. Staircase polygons are fully convex. A typical staircase polygon is shown in Fig. 1.

Mathematically, all the models require the calculation of the same object, the generalized partition function $G(y, z)$, where

$$G(y, z) = \sum_{m=1}^{\infty} A_m(y)\, z^m = \sum_{n=4}^{\infty} P_n(z)\, y^n \tag{1.1}$$

with

$$A_m(y) = \sum_{n=4}^{\infty} c_m^n y^n \qquad \text{and} \qquad P_n(z) = \sum_{m=1}^{\infty} c_m^n z^m \tag{1.2}$$

and c_m^n is the number of configurations with perimeter n and area m. The perimeter n has an associated perimeter fugacity y, and the area m an associated area fugacity z. Physically it is of interest to understand the behavior of the partition function $A_m(y)$ of vesicles of fixed area m as the perimeter fugacity y is varied and the partition function $P_n(z)$ of vesicles of fixed perimeter n as the area fugacity z is varied. The behavior of the partition functions for large vesicles is determined by the mathematical behavior of the generating function near its radius of convergence. Hence, it is of interest to study the generating function and especially study it near its radius of convergence. This is the aim of our work for the models of staircase and column-convex polygons.

Let $y_c(z)$ be the radius of convergence of the generating function $G(y, z)$ for fixed z:

$$y_c(z) = \lim_{n \to \infty} P_n(z)^{-1/n} \tag{1.3}$$

For vesicles this is related to the free energy per unit length of vesicles of fixed perimeter in the limit of large perimeters through the relation $y_c(z) = \exp[\beta f(z)]$, where

$$-\beta f(z) = \lim_{n \to \infty} \frac{1}{n} \log[P_n(z)] \tag{1.4}$$

Vesicles of fixed perimeter in solution are believed to undergo a phase transition as the osmotic pressure (area fugacity) is varied. The schematic shape of the radius of convergence $y_c(z)$ has been determined by Fisher *et al.*[15] and is shown in Fig. 2. The partially directed models considered in this paper have the same shaped radius-of-convergence curve. The free energy has a singularity at the "tricritical" point ($z = z_t = 1$, $y = y_t$). In the neighborhood of this point, below the line $y_c(z)$, the singular part of the generalized partition function is expected to have the asymptotic, or scaling, form[15,16]

$$G_{\text{sing}}(y, z) \sim (1-z)^{-\gamma_t} \hat{f}((y_t - y)(1-z)^{-\phi}) \tag{1.5}$$

with

$$\hat{f}(x) \sim \begin{cases} x^{-\gamma_t/\phi} & \text{as} \quad x \to \infty \\ 1 & \text{as} \quad x \to 0^+ \end{cases} \tag{1.6}$$

where ϕ is the tricritical crossover exponent and $\gamma_u = \gamma_t/\phi$. Note that sometimes the exponent notation $\alpha - 2$, which arises from the mapping of polygons to the free energy of some magnetic model, is used in place of the γ's used above.

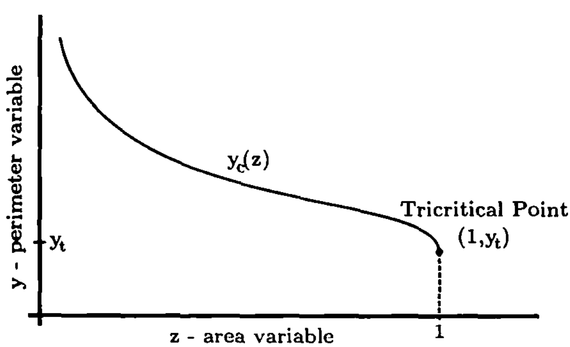

Fig. 2. Schematic plot of the radius of convergence of the generating function showing the tricritical point.

One may also consider the function $z_c(y)$, which is the radius of convergence of the generating function at fixed y. For $y \leqslant y_t$ it is expected that $z_c(y) = 1$. [For $y > y_t$ the function $z_c(y)$ is simply the inverse of the function $y_c(z)$.] The shape of the line $z_c(y)$ has the associated exponent ψ,

$$z_c(y) - z_t \sim (y - y_t)^{\psi} \tag{1.7}$$

which can be related simply to ϕ given the tricritical structure as $\psi = 1/\phi$.[16] Also, at fixed $y < y_t$ it is expected that the generating function has a droplet or condensation-like singularity.[15]

In this paper we shall be investigating the behavior of the generating functions especially near the tricritical point $(z, y) = (1, y_t)$. More precisely, we obtain the scaling form, as in (1.5) above, of the generating function for each model. For each of the models considered the generating function has a simple pole for $y > y_t$ on approaching $z_c(y)$ and the required droplet singularity for $y < y_t$.

It will be essential for solving the models to split the perimeter fugacity into two components, x and y, where y is the fugacity for the vertical perimeter bonds and x that for the horizontal perimeter bonds. In fact, for all these partially directed polygon models the "natural" variables are x, y, and z. Thus the object we calculate is

$$G(x, y, z) = \sum_{m} \sum_{n_1, n_2} c_m^{(n_1, n_2)} x^{n_1} y^{n_2} z^m \tag{1.8}$$

where $c_m^{(n_1, n_2)}$ is the number of polygons with n_1 horizontal perimeter bonds, n_2 vertical perimeter bonds, and area m. It will also be convenient to use the variables τ and ε, where

$$y = \exp(-\tau), \qquad z = \exp(-\varepsilon) \tag{1.9}$$

Before describing our work we briefly reiterate the previous contributions to these problems. The staircase polygons' area–perimeter generating function was obtained by Polya,[17] but he appears not to have published the proof. The perimeter-only generating function was first published by Gouyou–Beauchamps *et al.*[18] Other generating functions have also been found.[19] The column-convex polygon perimeter generating function was found by Delest[19] using algebraic languages and independently by Brak and Guttmann[2] using the Temperley method. The area–perimeter generating function was found by Brak and Guttmann[1] with a more compact form of the solution recently given by Bousquet-Mélou.[20] Various other generating functions have also been bound.[21–23]

Each of the above polygon models has a semicontinuous partner obtained by taking the continuum limit. The heights of the columns of the above polygons are all constrained to take on positive integer values. However, we can define an associated model where the heights of the columns are allowed to take on positive real values. These are then the semicontinuous staircase and semicontinuous column-convex polygon models. The continuum limit corresponds to allowing the lattice spacing in the vertical direction to tend to zero but keeping the physical height of the columns fixed. We investigate these models using the method introduced by Temperley[14] and utilized[1,2] in the solution of the fully discrete models. In the staircase problem this method allows the extraction of all the information required. In the column-convex case it gives us the full solution and some exponents. While in theory it might be possible to do the required asymptotics, and hence obtain the scaling function, we have found that this is not practical.

It will be shown that the discrete column-convex polygon generating function satisfies a set of nonlinear functional equations. One approach we use is to assume that a scaling function exists and, substituting a formal perturbation expansion into the functional equations, extract the exponents around the tricritical point. This has been done for the discrete column-convex model. However, a more rigorous approach is the following: We take the continuum limit of the functional equations, which become a set of coupled nonlinear differential equations. Using dominant balance ideas on the equivalent single nonlinear differential equation and matching the solution with the known solution at $z=1$, we extract the full scaling behavior of the semicontinuous model. The exponents obtained are in agreement with those obtained formally from the perturbation expansion in the discrete model.

Our major results for the scaling near the tricritical point can be summarized in the following equations. The generating function for staircase polygons can be written for $y \approx y_t$ and $z \approx 1$ as

$$\mathscr{G}_T(x, \tau, \varepsilon) \sim \tau + 2^{1/3} v^{-1/3} \frac{\mathrm{Ai}'(2^{-2/3} v^{2/3}(1-\sigma_T^2))}{\mathrm{Ai}(2^{-2/3} v^{2/3}(1-\sigma_T^2))} \tau \tag{1.10}$$

where

$$\sigma_T = \frac{x}{\tau} \qquad \text{and} \qquad v = \frac{2\tau}{\varepsilon} \tag{1.11}$$

The value of y_t is defined via $\sigma_T = 1$. The full solution for staircase polygons is given in Eq. (2.13) with the bonus of the asymptotic solution for all fixed $y \leqslant y_c(z)$ with $z \approx 1$ also given in Section 2. The above scaling

Table I. Exponents for Both the Partially Convex Vesicle Models, Staircase and Column-Convex Polygons, at the "Tricritical" Point

Exponent	γ_u	γ_t	ϕ	ψ
Value	$-1/2$	$-1/3$	$2/3$	$3/2$

form leads to the exponents given in Table I. For column-convex polygons, again for $y \approx y_t$ and $z \approx 1$, we have

$$\mathscr{G}_C(x, \tau, \varepsilon) \sim \frac{2}{17}(5 - 2\sqrt{2})\,\tau + \frac{2^2}{17^2}(19 + 6\sqrt{2})\,v^{-1/3}\,\frac{\mathrm{Ai}'(2^{-1}v^{2/3}(1-\sigma_C^2))}{\mathrm{Ai}(2^{-1}v^{2/3}(1-\sigma_C^2))}\,\tau \tag{1.12}$$

where

$$\sigma_C = \frac{2x}{\tau} \qquad \text{and} \qquad v = \frac{2\tau}{\varepsilon} \tag{1.13}$$

The value of y_t is defined via $\sigma_C = 1$. The exponents for column-convex polygons are also given in Table I and are the same as those for staircase polygons.

Abraham and collaborators have utilized and extended[24, 7] the mathematics of bar-graph polygons (see Fig. 1) in several contexts.[11-13] One context has been in modeling the wetting transition,[24, 7] while another has been in a low-temperature approximate theory of correlations in uniaxial ferromagnets.[11-13] In this second application the two-point spin–spin correlation function is written as a sum over solid-on-solid loops enclosing the two points. As originally formulated, the configurations considered are column-convex polygons. In an effort to produce a tractable problem Abraham[11] made an approximation to "center-of-mass" and relative coordinates. In this way he modified the mathematics so that the configurations considered were bar-graph polygons. More recently, Abraham and Upton reconsidered this bubble model[12, 13] in the context of the singularities in the susceptibility at the low-temperature first-order transition in Ising-like systems. Using the fact that the susceptibility is the sum over two-point correlations, they gave an expression for the susceptibility of the Ising system as a function of the field, surface tension, and magnetisation. This function was essentially the generating function of semicontinuous bar-graph polygons $\mathscr{G}_B(x, \tau, \varepsilon)$, which is given as

$$1 + \mathscr{G}_B(x, \tau, \varepsilon) = \frac{2}{\sigma_B}\,\frac{J_v(\sigma_B v)}{J_{v-1}(\sigma_B v)} \tag{1.14}$$

where

$$\nu = \frac{2\tau}{\varepsilon} \qquad \text{and} \qquad \sigma_B = \left(\frac{2}{\tau}\right)^{1/2} \tag{1.15}$$

Hence, it is interesting from several points of view to examine the original configurational states, which are column-convex polygons. Our major conclusion here is that, while the scaling behavior is of the same form in column-convex and bar-graph polygons, the nonuniversal amplitudes are different.

The layout of the paper is as follows. In Sections 2 and 3 we provide the solutions of the semicontinuous variants of staircase and column-convex polygons. In Section 4 the set of functional equations is derived for the discrete column-convex model and in Section 5 the exponents are found using the formal perturbation expansion. In Section 6 the semicontinuous limit of the functional equations is taken to give a nonlinear differential equation for the generating function of the column-convex model. In Section 7 this differential equation is solved in the scaling limit.

2. STAIRCASE POLYGONS

In this section we give the exact solution for the generating function of the semicontinuous analog of staircase polygons and as a consequence show that the scaling behavior extracted by the other methods of this paper gives the correct results.[10] The model is illustrated in Fig. 1a and we associate a fugacity x with horizontal steps, a fugacity $y = e^{-\tau}$ with vertical steps, and a fugacity $z = e^{-\varepsilon}$ with unit areas.

We solve for the generating function by adapting the Temperley method[14,1] to the continuous version of the problem. The generating function can be written as an integral over all polygons that have a fixed height of their leftmost column (see Fig. 3):

$$\mathscr{G}_T(x, \tau, \varepsilon) = \int_0^\infty T(r)\, dr \tag{2.1}$$

The major ingredient in the method of Temperley is to find a recurrence relation for $T(r)$, in this case an integral equation, and then solve for that generating function. Note that $T(r)$ depends also on τ, ε, and x. In the continuous case this procedure leads to a differential equation. This differential equation is one in the variable r rather than in one of the model parameters.

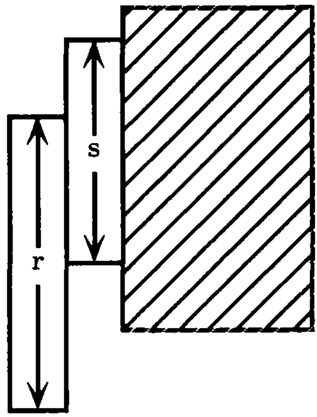

Fig. 3. The Temperley method for obtaining a recurrence relation for the generating function of a partially directed polygon problem. The idea is to consider that each polygon with leftmost column of height r can be constructed from all polygons of leftmost height s by adding a column of height r.

Considering the addition of a column of height r to a staircase polygon with leftmost column of height s, as in Fig. 3, gives us

$$T(r) = x^2 z^r y^{2r} + x^2 z^r \int_0^\infty ds\, T(s) f(r, s) \tag{2.2}$$

where

$$f(r, s) = (2\tau)^{-1} \exp(-2\tau r)\{\exp[\tau(r+s) - \tau\,|r-s|] - 1\} \tag{2.3}$$

It is more convenient to work with the function $g(r)$ defined as

$$g(r) = e^{\varepsilon r} e^{\tau r} T(r) \tag{2.4}$$

By differentiating the above integral equation, we obtain the differential equation

$$\frac{d^2 g}{dr^2} = (\tau^2 - x^2 e^{-\varepsilon r})\, g(r) \tag{2.5}$$

Making the substitutions $z = ae^{-\varepsilon r/2}$ and $h(z) = g(r)$, we obtain

$$z^2 \frac{d^2 h}{dz^2} + z \frac{dh}{dz} + \left(\frac{4x^2}{\varepsilon^2 a^2} z^2 - \frac{4\tau^2}{\varepsilon^2}\right) h(z) = 0 \tag{2.6}$$

This is Bessel's differential equation with

$$\nu = \frac{2\tau}{\varepsilon} \tag{2.7}$$

and

$$a = \frac{2x}{\varepsilon} \tag{2.8}$$

The solution is given by

$$h(z) = C_1 J_\nu(z) + C_2 J_{-\nu}(z) \tag{2.9}$$

with C_j being constants that depend on the boundary conditions implicit in the integral equation. One can show (analogously to ref. 6) that $C_2 = 0$ and hence we can solve the boundary condition

$$g(0) = x^2 \tag{2.10}$$

to obtain

$$g(r) = x^2 \frac{J_{2\tau/\varepsilon}((2x/\varepsilon)\, e^{-\varepsilon r/2})}{J_{2\tau/\varepsilon}(2x/\varepsilon)} \tag{2.11}$$

The boundary condition for $g'(r)$ can be written as

$$\mathscr{G}_T = x^{-2} g'(0) + \tau \tag{2.12}$$

and leads to

$$\mathscr{G}_T(x, \tau, \varepsilon) = \tau \left(1 - \sigma \frac{J_\nu'(\sigma\nu)}{J_\nu(\sigma\nu)}\right) \tag{2.13}$$

with

$$\sigma = \frac{x}{\tau} \quad \text{and} \quad \nu = \frac{2\tau}{\varepsilon} \tag{2.14}$$

For the sake of completeness we give the solution with $z = 1$:

$$\mathscr{G}_T(x, \tau, 0) = \tau - (\tau^2 - x^2)^{1/2} \tag{2.15}$$

Now the area fugacity occurs only in ν, while the horizontal fugacity comes into play only through σ. Considering the behavior of the Bessel functions, it can be seen that at fixed perimeter fugacities such that $\sigma \leqslant 1$ the generating function has singular behavior in the variable ν as the area fugacity z approaches 1 from below. For $\sigma > 1$ there is a pole in the generating function at some finite value of $\nu_c(\sigma)$ given by the solution of

$$J_{\nu_c}(\sigma \nu_c) = 0 \tag{2.16}$$

This behavior gives us the diagram in Fig. 2.

The change in behavior as a function of perimeter fugacity occurs at

$$\sigma(x, y) = 1 \tag{2.17}$$

or, if $x = y$, then $y \approx 0.56714$ at this point.

For large ν the Bessel functions can be asymptotically approximated by Airy functions and the generating function can be seen to behave as

$$\mathscr{G}_T(x, \tau, \varepsilon) \sim \tau + \left(\frac{1-\sigma^2}{\zeta}\right)^{1/2} \nu^{-1/3} \frac{\mathrm{Ai}'(\nu^{2/3}\zeta)}{\mathrm{Ai}(\nu^{2/3}\zeta)} \tau \tag{2.18}$$

where for $\sigma < 1$

$$\frac{2}{3}\zeta^{3/2} = \log \frac{1 + (1-\sigma^2)^{1/2}}{\sigma} - (1-\sigma^2)^{1/2} \tag{2.19}$$

This asymptotic expansion is uniform in σ. This allows the extraction of the critical exponents for the transition that occurs at $(\sigma, 1/\nu) = (1, 0)$. Near this point the variable ζ can be approximated by

$$\zeta \approx \frac{1-\sigma^2}{2^{2/3}} \tag{2.20}$$

Again for the sake of completeness, when $\sigma = 1$ the generating function is given by

$$\mathscr{G}_T(\tau, \tau, \varepsilon) \sim \tau - 6^{1/3} \frac{\Gamma(2/3)}{\Gamma(1/3)} \tau \nu^{-1/3} \tag{2.21}$$

Hence, the exponents at the critical point are $\gamma_u = -1/2$, $\gamma_t = -1/3$, $\phi = 2/3$, and $\psi = 3/2$.

This asymptotic behavior (2.18) is exactly the same as that extracted from the differential equation/scaling solution method.[10]

3. COLUMN-CONVEX POLYGONS

We present the solution of the generating function of the semicontinuous version of the vesicle model of column-convex polygons (also known as row-convex polygons) in this section. The solution is given in terms of hypergeometric functions ${}_0F_3$ and the asymptotic analysis of the solution would be a demanding task. This observation leads us to utilize the differential equation scaling solution to extract the exponents analytically in Sections 6 and 7. The model is illustrated in Fig. 1c and we associate a fugacity x with horizontal steps, a fugacity $y = e^{-\tau}$ with vertical steps, and a fugacity $z = e^{-\varepsilon}$ with unit areas.

We solve for the generating function by adapting the Temperley method[14, 1] as in the previous section. The generating function can be written as an integral over all polygons that have a fixed height of their leftmost column (see Fig. 3):

$$\mathscr{G}_C(x, \tau, \varepsilon) = \int_0^\infty C(r)\, dr \tag{3.1}$$

Considering the addition of a column of height r to a column-convex polygon with leftmost column of height s, as in Fig. 3, gives us

$$C(r) = x^2 z^r y^{2r} + x^2 z^r \int_0^\infty ds\, C(s) f(r, s) \tag{3.2}$$

where

$$\begin{aligned} f(r, s) = \tau^{-1} \exp(-2\tau r)\{\exp[\tau(r+s) - \tau\, |r-s|] - 1\} \\ + |r-s| \exp[-2\tau(r-s)\, \Theta(r-s)] \end{aligned} \tag{3.3}$$

The function $\Theta(\cdot)$ is the Heaviside step function.

It is more convenient to work with the function $g(r)$ defined (to avoid symbolic overload, we use similar symbols in this section to that of the previous redefined for the purposes of this section) as

$$g(r) = e^{(\varepsilon+\tau) r} C(r) \tag{3.4}$$

By differentiating the above integral equation, we can obtain the differential equation

$$\frac{d^4 g}{dr^4} - 2\tau^2 \frac{d^2 g}{dr^2} + (\tau^4 - 4\tau^2 x^2 e^{-\varepsilon r})\, g(r) = 0 \tag{3.5}$$

The boundary conditions from the integral equation are

$$g(0) = x^2(1 + \mathscr{K}_C) \tag{3.6}$$

and

$$g'(0) + \tau g(0) = x^2(\mathscr{G}_C + 2\tau \mathscr{K}_C) \tag{3.7}$$

where

$$\mathscr{K}_C(x, \tau, \varepsilon) = \int_0^\infty rC(r)\, dr \tag{3.8}$$

Making the substitutions $z = ae^{-\varepsilon r/2}$ and $h(z) = g(r)$, we obtain

$$\begin{aligned} &z^4 \frac{d^4h}{dz^4} + 6z^3 \frac{d^3h}{dz^3} + 7z^2 \frac{d^2h}{dz^2} + z \frac{dh}{dz} \\ &\quad = \frac{8\tau^2}{\varepsilon^2}\left(z^2 \frac{d^2h}{dz^2} + z \frac{dh}{dz}\right) + \left(\frac{64\tau^2 x^2}{\varepsilon^4 a^2} z^2 - \frac{16\tau^4}{\varepsilon^4}\right) h(z) = 0 \end{aligned} \tag{3.9}$$

This *cannot* be transformed into Bessel's differential equation, and so one must try a new series solution with

$$h_0(z) = z^\nu \sum_{m=0}^{\infty} h_m z^m \tag{3.10}$$

This indeed succeeds with the result that the function $A_\nu(z)$ defined as

$$A_\nu(z) = \sum_{m=0}^{\infty} \frac{(z/4)^{2m+\nu}}{[m!\, \Gamma(m+\nu+1)]^2} \tag{3.11}$$

with

$$\nu = \frac{2\tau}{\varepsilon} \tag{3.12}$$

and

$$a = \frac{8\tau x}{\varepsilon^2} \tag{3.13}$$

is a solution. If we write $a = \sigma\nu^2$, then

$$\sigma = \frac{2x}{\tau} \tag{3.14}$$

We notice immediately that the function $\sigma(x, y)$ is different in the column-convex case than in the staircase model. The function A_ν is a hypergeometric function:

$$A_\nu(z) = \frac{z^\nu}{[\Gamma(\nu+1)]^2}\, {}_0F_3\left(\nu+1, \nu+1, 1; \left(\frac{z}{4}\right)^2\right) \tag{3.15}$$

This gives us two independent solutions with A_ν and $A_{-\nu}$. However, as we have a fourth-order differential equation, four independent solution are required. These are found from the ansatz

$$h_1(z) = (\log z)\, A_\nu(z) + \sum_{m=0}^{\infty} u_m \frac{(z/4)^{2m+\nu}}{[m!\, \Gamma(m+\nu+1)]^2} \tag{3.16}$$

by solving for u_m by substituting into the differential equation. The u_m are given by

$$u_m = -\sum_{k=1}^{m} \left(\frac{1}{k} + \frac{1}{k+\nu}\right) \tag{3.17}$$

This gives us two further solutions (the second has $\nu \to -\nu$) as

$$(\log z)\, A_\nu(z) + B_\nu(z) \tag{3.18}$$

with

$$B_\nu(z) = -\sum_{m=0}^{\infty} \left[\sum_{k=1}^{m} \left(\frac{1}{k} + \frac{1}{k+\nu}\right)\right] \frac{(z/4)^{2m+\nu}}{[m!\, \Gamma(m+\nu+1)]^2} \tag{3.19}$$

As with the staircase problem, one can dismiss the $-\nu$ solutions immediately. However, in this case that still leaves us with two independent solutions. The full solution is then given by

$$h(z) = C_1 A_\nu(z) + C_2[(\log z)\, A_\nu(z) + B_\nu(z)] \tag{3.20}$$

with C_j being the constants that depend on the boundary condition implicit in the integral equation.

It is now possible to use the boundary conditions (3.6), (3.7) with the definition (3.8) to find the constants C_1 and C_2 and hence the generating function $\mathscr{G}_C(x, \tau, \varepsilon)$. To write down the solution, we first define several functions related to A_ν and B_ν. Let

$$a_m = \frac{1}{[m!\, \Gamma(m+\nu+1)]^2} \tag{3.21}$$

and $b_m = u_m a_m$. Then we define

$$A_\nu^{(j)}(z) = \sum_{m=0}^{\infty} \frac{a_m (z/4)^{2m+\nu}}{[2(m+\nu+1)]^j} \tag{3.22}$$

and

$$B_\nu^{(j)}(z) = \sum_{m=0}^{\infty} \frac{b_m (z/4)^{2m+\nu}}{[2(m+\nu+1)]^j} \tag{3.23}$$

The constants C_k are, subsequentially,

$$C_1 = \frac{R_1(\sigma, \nu)}{R_2(\sigma, \nu)} C_2 \tag{3.24}$$

and

$$C_2 = \frac{x^2 R_2(\sigma, \nu)}{R_1(\sigma, \nu)[A_\nu(\sigma\nu^2) - (\sigma^2\nu^2/4) A_\nu^{(2)}(\sigma\nu^2)] + R_2(\sigma, \nu) R_4(\sigma, \nu)} \tag{3.25}$$

with

$$\begin{aligned} R_1(\sigma, \nu) = {} & \frac{\sigma^2\nu^3}{2} [(\log \sigma\nu^2) A_\nu^{(2)}(\sigma\nu^2) + B_\nu^{(2)}(\sigma\nu^2) - 2A_\nu^{(3)}(\sigma\nu^2)] \\ & + \frac{\sigma^2\nu^2}{4} [(\log \sigma\nu^2) A_\nu^{(1)}(\sigma\nu^2) - A_\nu^{(2)}(\sigma\nu^2) + B_\nu^{(1)}(\sigma\nu^2)] \\ & + [A_\nu(\sigma\nu^2) + \sigma\nu^2(\log \sigma\nu^2) A'_\nu(\sigma\nu^2) + \sigma\nu^2 B'_\nu(\sigma\nu^2)] \\ & - \nu[(\log \sigma\nu^2) A_\nu(\sigma\nu^2) + B_\nu(\sigma\nu^2)] \end{aligned} \tag{3.26}$$

$$R_2(\sigma, \nu) = \nu A_\nu(\sigma\nu^2) - \sigma\nu^2 A'_\nu(\sigma\nu^2) - \frac{\sigma^2\nu^2}{4} A_\nu^{(1)}(\sigma\nu^2) - \frac{\sigma^2\nu^3}{2} A_\nu^{(2)}(\sigma\nu^2) \tag{3.27}$$

$$R_3(\sigma, \nu) = [(\log \sigma\nu^2) A_\nu^{(1)}(\sigma\nu^2) - A_\nu^{(2)}(\sigma\nu^2) + B_\nu^{(1)}(\sigma\nu^2)] \tag{3.28}$$

and

$$\begin{aligned} R_4(\sigma, \nu) = {} & (\log \sigma\nu^2) \left[A_\nu(\sigma\nu^2) - \frac{\sigma^2\nu^2}{4} A_\nu^{(2)}(\sigma\nu^2) \right] \\ & + \left[B_\nu(\sigma\nu^2) - \frac{\sigma^2\nu^2}{4} B_\nu^{(2)}(\sigma\nu^2) \right] + \frac{\sigma^2\nu^2}{2} A_\nu^{(3)}(\sigma\nu^2) \end{aligned} \tag{3.29}$$

where $A'(B')$ refers to the derivative of $A(B)$ with respect to z.

The generating function is, finally, given as

$$\mathscr{G}_C(x, \tau, \varepsilon) = \frac{2x^2}{\varepsilon} \frac{R_1(\sigma, \nu) B_\nu(\sigma\nu^2) + R_2(\sigma, \nu) R_3(\sigma, \nu)}{R_1(\sigma, \nu)[A_\nu(\sigma\nu^2) - (\sigma^2\nu^2/4) A_\nu^{(2)}(\sigma\nu^2)] + R_2(\sigma, \nu) R_4(\sigma, \nu)} \tag{3.30}$$

If $\varepsilon = 0$, this simplifies to

$$\mathscr{G}_C(x, \tau, 0) = \frac{2\tau x^3[x(\lambda_+ - \lambda_-) - 2(\lambda_+ + \tau)(\lambda_- + \tau)]}{(\lambda_+ - \lambda_-)[x^4 + x^2(\lambda_+ + \lambda_- + 2\tau)^2 - (\lambda_+ + \tau)^2 (\lambda_- + \tau)^2]} \tag{3.31}$$

with

$$\lambda_{\pm} = (\tau^2 \pm 2x\tau)^{1/2} \tag{3.32}$$

and expanding around $\sigma = 1$, with $\varepsilon = 0$, we have

$$\mathscr{G}_C\left(\frac{\tau\sigma}{2}, \tau, 0\right) = \left(\frac{10 - 4\sqrt{2}}{17}\right)\tau - \left(\frac{76 + 24\sqrt{2}}{289}\right)\tau(1-\sigma)^{1/2} \tag{3.33}$$

The critical point is given by $\sigma = 1$, although we reiterate that this translates to a different relationship between the fugacities, compared to staircase polygons, as

$$\tau = 2x \tag{3.34}$$

The perimeter generating function has the same type of singularity as in the staircase problem with a square root behavior ($\gamma_u = -1/2$) on approaching $\sigma = 1$ with $\varepsilon = 0$.

Because of the complexity of the solution, we find it advantageous to sidestep the direct asymptotic analysis of the full generating function by utilizing the differential equation/scaling solution method[10] to obtain the scaling behavior near $(\varepsilon, \sigma) = (0, 1)$ in Sections 6 and 7. First, however, we examine the discrete model.

4. FUNCTIONAL EQUATIONS

We follow the method of Prellberg and Brak[10] to derive a set of coupled functional equations for the generating function for column-convex polygons. Here, it is convenient to write this generating function in the variables $u = x^2$ and $v = y^2$, a natural choice, as there are always even numbers of horizontal and vertical perimeter bonds in column-convex polygons. It is further necessary to introduce two additional generating variables λ and μ which count the height of the leftmost and rightmost columns, respectively. We will show now that $G(u; \lambda, \mu) = G(u, v, z; \lambda, \mu)$ satisfies

$$\begin{aligned} G(u; \lambda, \mu) = {} & \lambda[1 + G_\mu(zu; \lambda, 1) - G(zu; \lambda, 1)]\, zu[v\mu + G_\lambda(u; 1, \mu)] \\ & + \lambda G(zu; \lambda, 1)\, v\mu + 2\lambda G(zu; \lambda, 1)\, G(u; 1, \mu) \end{aligned} \tag{4.1}$$

where we denote partial differentiation with a subscript, e.g.,

$$G_\mu(u; \lambda, \mu) = \frac{\partial}{\partial \mu} G(u; \lambda, \mu) \tag{4.2}$$

and drop the second and third arguments of the generating function for the sake of readability.

This equation can be best understood by using a graphical representation (see Fig. 4). The general idea is to partition the set of all polygons into disjoint subsets, and to give construction rules for the polygons in these subsets, which then are expressed as functional equations of the respective generating functions.

The partition we choose is characterized by the leftmost overlap of height one between two neighboring columns in a polygon. We now explain the diagrams in Fig. 4 one by one and derive their generating function representation.

The first diagram represents the case with no overlap of height one. Then the polygon can be written as an "inflated" polygon, which can be obtained by increasing the size of a column-convex polygon (symbolized by a square) by adding one area element to each column (symbolized by a square with an attached black bar on top). In terms of the generating func-

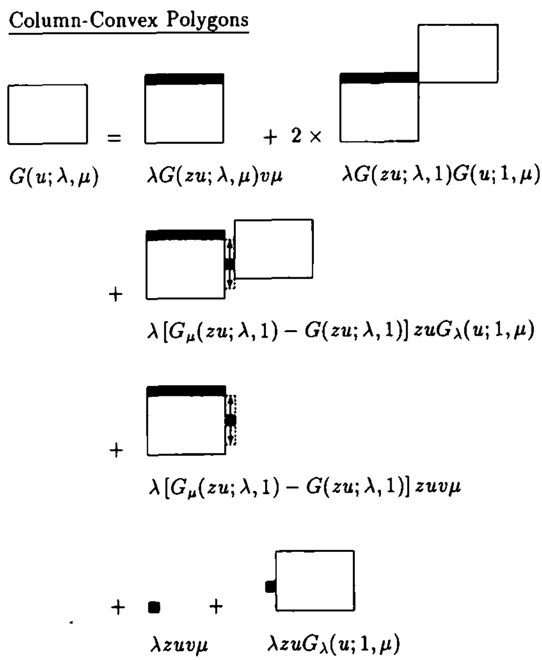

Fig. 4. Diagrammatic form of the functional equation. The clear square corresponds to the generating function G, the black regions are parts added to G. The arrows indicate summation over the height of the indicated region.

tion, the addition of an area element for every horizontal step means that u gets replaced by zu, and the increase of the number of vertical steps and the left and right heights of the polygon leads to a multiplication by $\lambda v \mu$. Therefore, the generating function G_1 for an inflated polygon is given by

$$G_1(u; \lambda, \mu) = \lambda G(zu; \lambda, \mu)\, v\mu \tag{4.3}$$

If there is an overlap of height one, then the part of the polygon to the left of this overlap is again an inflated polygon (unless, of course, the polygon starts with a column of height one, which we consider below). This inflated polygon gets concatenated to another polygon, either directly at their respective corners or with a joining single square between them (unless the leftmost overlap of height one happens to be at the rightmost column, which is also considered below).

The second diagram represents the concatenation at the corners. This concatenation sums over all possible right heights of the inflated polygon ($\mu = 1$) and all the possible left heights of the second one ($\lambda = 1$). The concatenation also reduces the number of total vertical steps by two, leading to a factor of v^{-1}, so that we get

$$G_2(u; \lambda, \mu) = G_1(u; \lambda, 1)\, v^{-1} G(u; 1, \mu) = \lambda G(zu; \lambda, 1)\, G(u; 1, \mu) \tag{4.4}$$

The third diagram represents the concatenation of an inflated column-convex polygon with a column-convex polygon by a single square. Naturally, there is multiplicity due to the various possible positions of the middle square. The square may be attached to the right polygon everywhere, which can be written as $(\partial/\partial\lambda)\, G(u; \lambda, \mu)|_{\lambda=1}$. However, the left polygon gets attached everywhere *except at the top and bottom positions* (which have already been counted as a subset of configurations in G_2), written as

$$\left.\frac{\partial}{\partial\mu}\frac{1}{\mu^2}\, G_1(u; \lambda, \mu)\right|_{\mu=1}$$

Multiplying these terms to the middle square gives

$$\begin{aligned} G_3(u; \lambda, \mu) &= \left.\frac{\partial}{\partial\mu}\frac{1}{\mu^2}\, G_1(u; \lambda, \mu)\right|_{\mu=1} \left.\frac{zu}{v}\frac{\partial}{\partial\lambda}\, G(u; \lambda, \mu)\right|_{\lambda=1} \\ &= \lambda[G_\mu(zu; \lambda, 1) - G(zu; \lambda, 1)]\, zuG_\lambda(u; 1, \mu) \end{aligned} \tag{4.5}$$

Finally, we turn to the exceptional cases mentioned above. Here, the left or right polygon is missing, leading to the generating functions for the remaining three diagrams in Fig. 4:

$$G_4(u;\lambda,\mu)=\lambda[G_\mu(zu;\lambda,1)-G(zu;\lambda,1)]\,zu\mu \tag{4.6}$$

$$G_5(u;\lambda,\mu)=\lambda zu\mu \tag{4.7}$$

$$G_6(u;\lambda,\mu)=\lambda zuG_\lambda(u,v,z;1,\mu) \tag{4.8}$$

Summing up $G=G_1+2G_2+G_3+G_4+G_5+G_6$, we get Eq. (4.1).

We can transform this functional-differential equation into a set of functional equations by partially differentiating (4.1) with respect to λ and μ and setting $\lambda=\mu=1$. This leads to

$$g=\{1+G_\mu-G\}\,zu\{v+g_\lambda\}+\{v+2g\}\,G \tag{4.9a}$$

$$g_\lambda=g+\{G_{\lambda\mu}-G_\lambda\}\,zu\{v+g_\lambda\}+\{v+2g\}\,G_\lambda \tag{4.9b}$$

$$g_\mu=\{1+G_\mu-G\}\,zu\{v+g_{\lambda\mu}\}+\{v+2g_\mu\}\,G+vG_\mu \tag{4.9c}$$

$$g_{\lambda\mu}=g_\mu+\{G_{\lambda\mu}-G_\lambda\}\,zu\{v+g_{\lambda\mu}\}+\{v+2g_\mu\}\,G_\lambda+vG_{\lambda\mu} \tag{4.9d}$$

where

$$\begin{aligned} g(u,v,z)&=G(u;1,1) \qquad & g_\lambda(u,v,z)&=G_\lambda(u;1,1)\\ g_\mu(u,v,z)&=G_\mu(u;1,1) \qquad & g_{\lambda\mu}(u,v,z)&=G_{\lambda\mu}(u;1,1)\end{aligned} \tag{4.10}$$

and

$$\begin{aligned} G(u,v,z)&=g(uz,v,z) \qquad & G_\lambda(u,v,z)&=g_\lambda(uz,v,z)\\ G_\mu(u,v,z)&=g_\mu(uz,v,z) \qquad & G_{\lambda\mu}(u,v,z)&=g_{\lambda\mu}(uz,v,z)\end{aligned} \tag{4.11}$$

By the symmetry of the configurations we must have $g_\mu=g_\lambda$ and thus there are actually only three independent equations in the three unknown functions g, g_λ, and $g_{\lambda\mu}$. Choosing the first three equations leads to a final set of three coupled nonlinear functional equations,

$$g=\{1+G_\lambda-G\}\,zu\{v+g_\lambda\}+\{v+2g\}\,G \tag{4.12a}$$

$$g_\lambda=g+\{G_{\lambda\mu}-G_\lambda\}\,zu\{v+g_\lambda\}+\{v+2g\}\,G_\lambda \tag{4.12b}$$

$$g_\lambda=\{1+G_\lambda-G\}\,zu\{v+g_{\lambda\mu}\}+\{v+2g_\lambda\}\,G+vG_\lambda \tag{4.12c}$$

5. PERTURBATION EXPANSION

Using an asymptotic expansion around $z=1$, one can use (4.12) to derive a set of exponents at the tricritical point.[10] First, we note that setting $z=1$ results in a set of algebraic equations which can be solved explicitly for $A(u,v)=g(u,v,1)$, $A_1(u,v)=g_\lambda(u,v,1)$, and $A_2(u,v)=g_{\lambda\mu}(u,v,1)$,

$$A = A(v+2A) + (1 + A_1 - A)\, u(v + A_1) \tag{5.1a}$$

$$A_1 = A + A_1(v+2A) + (A_2 - A_1)\, u(v + A_1) \tag{5.1b}$$

$$A_1 = A(v+2A_1) + (1 + A_1 - A)\, u(v + A_2) + A_1 v \tag{5.1c}$$

One can transform this system to get algebraic equations for A, A_1, and A_2. We give the result for $A(u, u)$:

$$\begin{aligned} 0 = &-(u-1)^4 u^2 + (u^3 - 7u^2 + 3u - 1)(u-1)^3 A \\ &+ 2(2u^3 - 11u^2 + 10u - 4)(u-1)^2 A^2 \\ &+ (u-1)(5u^3 - 35u^2 + 47u - 21)\, A^3 \\ &+ (2u^3 - 23u^2 + 38u - 18)\, A^4 \end{aligned} \tag{5.2}$$

which is the perimeter generating function, Eq. (18) in ref. 1. $A(u, u)$ has a square-root singularity at

$$u_c = 3 - 2\sqrt{2} \tag{5.3}$$

leading to a value of

$$\gamma_u = -\tfrac{1}{2} \tag{5.4}$$

As described in ref. 10, we can now compute the crossover exponent ϕ by using an asymptotic expansion in $z = \exp(-\varepsilon)$. Expanding up to first order in ε, we write

$$g(u, v, z) = A(u, v) + \varepsilon B(u, v) \tag{5.5a}$$

$$g_\lambda(u, v, z) = A_1(u, v) + \varepsilon B_1(u, v) \tag{5.5b}$$

$$g_{\lambda\mu}(u, v, z) = A_2(u, v) + \varepsilon B_2(u, v) \tag{5.5c}$$

so that

$$G(u, v, z) = A(u, v) + \varepsilon(B(u, v) - uA_u(u, v))$$

$$\text{with} \qquad A_u(u, v) = \frac{\partial}{\partial u} A(u, v) \tag{5.6}$$

and correspondingly for G_λ and $G_{\lambda\mu}$. This leads to the following system of three equations:

$$\begin{aligned} B + uA_u = {} & (1 + A_1 - A)\, u(B_1 + uA_{1u}) + (B_1 - B)\, u(v + A_1) \\ & + A(2B + 2uA_u) + B(v + 2A) \end{aligned} \tag{5.7a}$$

$$B_1 + uA_{1u} = (A_2 - A_1)\, u(B_1 + uA_{1u}) + (B_2 - B_1)\, u(v + A_1) + B + uA_u + A_1(2B + 2uA_u) + B_1(v + 2A) \tag{5.7b}$$

$$B_1 + uA_{1u} = (1 + A_1 - A)\, u(B_2 + uA_{2u}) + (B_1 - B)\, u(v + A_2) + A(2B_1 + 2uA_{1u}) + B(v + 2A_1) + B_1 v. \tag{5.7c}$$

This system of equations is linear in B, B_1, and B_2, with a determinant $D(u, v)$ fulfilling (again, we give the result for $u = v$ only)

$$\begin{aligned} 0 = &-4(u^2 - 6u + 1)^2 (u+1)^4 (u-1)^{10} \\ &+ (u + 19)(u^2 - 6u + 1)(u+1)^2 (u-1)^6 D^2 \\ &- 3(u^2 - 6u + 1)(u+1)^2 (u-1)^3 D^3 \\ &+ (2u^3 - 23u^2 + 38u - 18) D^4 \end{aligned} \tag{5.8}$$

In the above we have inserted the expressions for A, A_1, and A_2. Then B can be written as

$$B(u, v) = \frac{\gamma_0(u, v) + \gamma_1(u, v)\, A_u(u, v) + \gamma_2(u, v)\, A_{1u}(u, v) + \gamma_3(u, v)\, A_{2u}(u, v)}{D(u, v)} \tag{5.9}$$

with $\gamma_i(u, v)$ being multinomials in u and v. Since $D(u, u)$ has a square root singularity at $u_c = 3 - 2\sqrt{2}$, then $B(u, u)$ diverges at u_c with exponent $\gamma_u^{(1)} = 1$, provided that no cancellations occur, which needs to be checked explicitly. For this, we give $B(u, u)$ as the solution of an algebraic equation,

$$\begin{aligned} 0 = &\, u^4(u-1)^4 (2u^9 - 15u^8 + 8u^7 + 60u^6 \\ &- 4u^5 - 106u^4 - 56u^3 + 60u^2 - 14u + 1) \\ &+ u^2(u-1)^4 (u+1)(u^2 - 6u + 1)(2u^{10} - 21u^9 + 61u^8 - 72u^7 \\ &+ 32u^6 + 230u^5 - 282u^4 - 480u^3 + 342u^2 - 73u + 5)\, B \\ &+ (u-1)^2 (u+1)^2 (u^2 - 6u + 1)^2 (4u^{12} - 52u^{11} + 157u^{10} + 162u^9 \\ &- 973u^8 - 60u^7 + 2687u^6 - 2902u^5 + 1629u^4 \\ &- 988u^3 + 364u^2 - 64u + 4)\, B^2 \\ &- 4u(u-1)^2 (u+1)^3 (u^2 - 6u + 1)^3 (24u^7 - 190u^6 + 261u^5 + 699u^4 \\ &- 1615u^3 + 885u^2 - 168u + 24)\, B^3 \\ &- 4u(u+1)^4 (u^2 - 6u + 1)^4 (2u - 23u^2 + 38u - 18)^2 B^4 \end{aligned} \tag{5.10}$$

One can now check that $\gamma_u^{(1)}$ is indeed equal to 1, and we can read off the crossover exponent ϕ via its relation to the *gap exponent* $\Delta = \gamma_u^{(1)} - \gamma_u$. We have

$$\phi = \frac{1}{\Delta} = \frac{2}{3} \qquad \text{and thus} \qquad \gamma_t = \phi \gamma_u = -\frac{1}{3} \tag{5.11}$$

We emphasize that this derivation uses the assumed existence of an asymptotic expansion at the critical line $z = 1$ and interprets the exponents within an assumed scaling ansatz.

6. CONTINUUM LIMIT

The semicontinuous column-convex model solved in Section 3 can be obtained by taking the continuum limit of the lattice model. To see how this occurs, we can write the lattice generating function in the form

$$\begin{aligned} g(u, v, z) &\\ = \sum_{n=1}^{\infty} u^n \sum_{k_1=1}^{\infty} \cdots \sum_{k_n=1}^{\infty} \sum_{m_1=1-k_2}^{k_1-1} \cdots \sum_{m_{n-1}=1-k_n}^{k_{n-1}-1} \exp[-\mathscr{H}_n(k_1, m_1, ..., k_n)] \end{aligned} \tag{6.1}$$

where

$$\mathscr{H}_n = \sum_{i=1}^{n} \{\tau \mathscr{P}(k_{i-1}, m_{i-1}, k_i) + \varepsilon k_i\}, \qquad k_0 = 0 \tag{6.2}$$

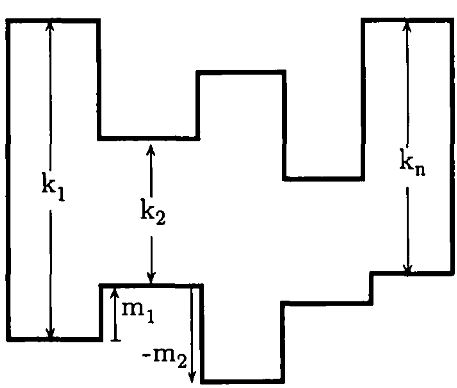

Fig. 5. Length labeling of the lattice column-convex model.

and $\mathscr{P}(k_{i-1}, m_{i-1}, k_i)$ is the length of the perimeter between columns i and $i+1$. The labeling of the lengths is shown in Fig. 5. Note that the number of summation signs associated with a configuration with n columns is $2n-1$. The generating function for the semicontinuous column-convex model is

$$\mathscr{G}_C(\sqrt{u}, \tau, \varepsilon) = \sum_{n=1}^{\infty} u^n \int_0^{\infty} dr_1 \cdots \int_0^{\infty} dr_n \int_{-r_2}^{r_1} ds_1 \cdots \int_{-r_n}^{r_{n-1}} ds_{n-1} \times \exp[-\mathscr{H}_n(r_1, s_1, ..., r_n)] \tag{6.3}$$

We can now obtain this generating function from the lattice model by explicitly inserting the lattice spacing a into the lattice generating function and taking the continuum limit $a \to 0$. This gives

$$\mathscr{G}_C(\sqrt{u}, \tau, \varepsilon) = \lim_{a \to 0} \frac{1}{a} g(a^2 u, v^a, z^a) \tag{6.4}$$

where we use $\lim_{a \to 0} \sum_m af(am) = \int dr\, f(r)$, $r = am$, on each of the summations appearing in (6.1). Equation (6.4) shows that

$$\frac{1}{a} g(a^2 u, v^a, z^a) = O(1) \tag{6.5}$$

as $a \to 0$. Extending (6.1) to the generating function containing the left and right column height generating variables λ and μ, we can show that

$$\frac{\partial}{\partial \lambda} g(a^2 u, v^a, z^a; \lambda, \mu) = O(1) \tag{6.6}$$

$$\frac{\partial^2}{\partial \lambda\, \partial \mu} ag(a^2 u, v^a, z^a; \lambda, \mu) = O(1) \tag{6.7}$$

as $a \to 0$.

We now use the set of functional equations for the column-convex lattice model to obtain a set of coupled nonlinear differential equations for the semicontinuous model. By multiplying or dividing by a, we can write the functional equations (4.9) as

$$\frac{g}{a} = \left\{1 + G_\mu - a\frac{G}{a}\right\} z^a au\{v^a + g_\lambda\} + \left\{v^a + 2a\frac{g}{a}\right\} \frac{G}{a} \tag{6.8a}$$

$$g_\lambda = a\frac{g}{a} + \{G_{\lambda\mu} - G_\lambda\} z^a a^2 u\{v^a + g_\lambda\} + \left\{v^a + 2a\frac{g}{a}\right\} G_\lambda \tag{6.8b}$$

$$g_\mu=\left\{1+G_\mu-a\frac{G}{a}\right\}z^a a^2u\{v^a+g_{\lambda\mu}\}+\{v^a+2g_\mu\}\,a\frac{G}{a}+v^aG_\mu \qquad (6.8c)$$

$$ag_{\lambda\mu}=ag_\mu+a\{G_{\lambda\mu}-G_\lambda\}\,z^a a^2u\{v^a+g_{\lambda\mu}\}+a\{v^a+2g_\mu\}\,G_\lambda+v^aaG_{\lambda\mu} \qquad (6.8d)$$

where we have replaced v by v^a, z by z^a, and u by a^2u (but not shown it in the arguments of the generating functions, for clarity). Let $z=\exp(-\varepsilon)$ and $v=\exp(-\eta)$; then Taylor expanding for small a the explicit factors of z^a and v^a in (6.8) and using

$$G(a^2u,v^a,z^a)=g(z^aa^2u,v^a,z^a)=g(a^2u,v^a,z^a)-a^3u\varepsilon g'+O(a^4)$$

(and similarly for G_λ, G_μ, and $G_{\lambda\mu}$) gives

$$\varepsilon u\frac{g'}{a}=u(1+g_\mu)(1+g_\lambda)+2\frac{g^2}{a^2}-\eta\frac{g}{a}+O(a) \qquad (6.9a)$$

$$\varepsilon ug'_\lambda=\frac{g}{a}+uag_{\lambda\mu}(1+g_\lambda)+2g_\lambda\frac{g}{a}-\eta g_\lambda+O(a) \qquad (6.9b)$$

$$\varepsilon ug'_\mu=\frac{g}{a}+uag_{\lambda\mu}(1+g_\mu)+2g_\mu\frac{g}{a}-\eta g_\mu+O(a) \qquad (6.9c)$$

$$\varepsilon uag'_{\lambda\mu}=g_\mu+g_\lambda-\eta ag_{\lambda\mu}+ua^2g^2_{\lambda\mu}+2g_\lambda g_\mu+O(a) \qquad (6.9d)$$

where the prime denotes differentiation with respect to the first (i.e., u) argument of the function. Note the explicit symmetry of the equations for g_μ and g_λ showing $g_\lambda=g_\mu$. Thus we need only three of the equations. Now, take $a\to 0$; using (6.5)–(6.7) gives

$$\rho t\frac{dF_0}{dt}=tF_1^2+2F_0^2+3F_0+1 \qquad (6.10a)$$

$$\rho t\frac{dF_1}{dt}=tF_1F_2+F_1+2F_0F_1-F_0 \qquad (6.10b)$$

$$\rho t\frac{dF_2}{dt}=tF_2^2-F_2-2F_1+2F_1^2 \qquad (6.10c)$$

where

$$\rho=\frac{\varepsilon}{\eta},\qquad t=\frac{u}{\eta^2},\qquad F_0(t)=\frac{1}{\eta}\hat{g}(\eta^2t,\eta,\varepsilon)-1,\qquad F_1=\hat{g}_\lambda+1,\qquad F_2=\eta\hat{g}_{\lambda\mu} \qquad (6.11)$$

and

$$\hat{g}(u, \eta, \varepsilon) = \lim_{a \to 0} \frac{1}{a} g(a^2 u, v^a, z^a), \qquad \hat{g}_\lambda = \lim_{a \to 0} g_\lambda, \qquad \hat{g}_{\lambda\mu} = \lim_{a \to 0} a g_{\lambda\mu} \tag{6.12}$$

As a check on these equations, we can solve for the perimeter-only generating function. This corresponds to $z = 1$ or $\varepsilon = 0$. Thus, putting $\rho = 0$ in (6.10) and eliminating F_1 and F_2 gives the following quartic algebraic equation for $F_{00} = F_0(\rho = 0)$:

$$(18 + t) F_{00}^4 + 51 F_{00}^3 + 53 F_{00}^2 + 24 F_{00} + 4 = 0 \tag{6.13}$$

We do not give the expression for the physical branch from (6.13), as it rather long; however, Taylor expanding gives

$$F_{00} = -1 + t + 4t^2 + 33t^3 + 334t^4 + 3766t^5 + O(t^6) \tag{6.14}$$

As a check, if the alternative and apparently quite different expression (3.31) is also Taylor expanded, exactly the same result is obtained. A study of the physical branch of (6.13) shows that

$$\frac{\hat{g}}{\eta} \sim \frac{1}{17}(5 - 2\sqrt{2}) - \frac{2^2}{17^2}(12 + 19\sqrt{2}) \left(\frac{1}{16} - t\right)^{1/2} \quad \text{as} \quad t \to \frac{1}{16} \tag{6.15}$$

and thus we have that

$$t_c = \tfrac{1}{16}, \qquad \gamma_u = -\tfrac{1}{2} \tag{6.16}$$

Note that $t_c = 1/16$ is equivalent to $2x = \tau$ (or $2x = -\log y$), as $\eta = 2\tau$ and $u = x^2$.

7. SCALING FUNCTION

We now proceed to compute the exact scaling function for the semi-continuous column-convex model. The three nonlinear equations (6.10) can be reduced to a single nonlinear equation for F_0 by eliminating F_1 and F_2. This produces a 381-term nonlinear equation which is quadratic in the third derivative. The equation for F_0 begins and ends as follows:

$$4t^{10}\rho^8 \left(\frac{dF_0}{dt}\right)^2 \left(\frac{d^3F_0}{dt^3}\right)^2 + \cdots (379 \text{ terms}) \cdots + 4 = 0 \tag{7.1}$$

Putting $\rho = 0$ into (7.1) does give (6.13) as required. The form of the solution obtained in Section 3 suggests (7.1) might be an instance of a generalized Ricatti equation;[25] however, this would require it to be linear in the third derivative. We were unable to transform the equation into the required form. However, should this be possible, the equation could then be solved explicitly, as it can be linearized.

If only the scaling behavior is required, then it is not necessary to solve (7.1) explicitly, but only *asymptotically* as $\rho \to 0$. Following ref. 10, we first change variables to shift the singular point to the origin. From (6.15) and (6.11) we let

$$F_0 = \hat{F}_0 - \tfrac{2}{17}(6+\sqrt{2}), \qquad t = \hat{t} + \tfrac{1}{16} \tag{7.2}$$

which gives, in expanded form, a 2548-term nonlinear differential equation.

We now take the important step of looking for a generalized homogeneous solution. To this end we change independent and dependent variables to

$$\hat{F}_0 = \rho^q H, \qquad \hat{t} = \rho^p w \tag{7.3}$$

which produces the following equation for $H(w)$:

$$w^{20}\rho^{8+10p+4q}\left(\frac{dH}{dw}\right)^2\left(\frac{d^3H}{dw^3}\right)^2 + \cdots (2546 \text{ terms}) \cdots + \rho^p w = 0 \tag{7.4}$$

Note that *all* the terms of the equation are multiplied by some power of ρ which is a linear combination of p and q, plus some constant. This equation does not have a solution independent of ρ as desired; however, it is dominated by several terms which give rise to such a solution. To see this, we use the principle of dominant balance.[26] This tells us that the dominant asymptotic form of H, H_0, is obtained by those terms which dominate the differential equation as $\rho \to 0$.

Let the powers of ρ of each term be d_i, $i = 1,..., 2548$. Clearly the set of terms with the *equally smallest* d_i dominates all the others: if there are m equally smallest terms, then

$$d_{i_1} = d_{i_2} = \cdots = d_{i_m} < d_{i_{m+1}} \leqslant d_{i_{m+2}} \leqslant \cdots$$

Thus, the problem reduces to finding the values of p and q which give a nonempty set $\chi = \{d_{i_1}, d_{i_2},..., d_{i_m}\}$. As each d_i is of the form $d_i = c_{i_1} p + c_{i_2} q + c_{i_3}$, where the c_i's are known constants, the problem becomes that of finding the sets of consistent linear simultaneous equations for which χ is nonempty. In general there will be many solutions to this problem; we can *uniquely* pick one of these solutions by requiring that the solution of the resulting differential equation *asymptotically match* the known $\rho = 0$ solution [Eq. (6.15)].

We find that

$$p = \tfrac{2}{3}, \qquad q = \tfrac{1}{3} \tag{7.5}$$

Remarkably, there are only three elements in the set χ and hence all the 2548 terms are dominated by only three. Thus the solution of (7.4) is asymptotic to the solution of a three-term differential equation

$$\frac{dH_0}{dw} = cw + bH_0^2 \tag{7.6}$$

where

$$c = \frac{2^7}{17^2}(19 + 6\sqrt{2}) \qquad \text{and} \qquad b = 4(19 - 6\sqrt{2}) \tag{7.7}$$

This equation is a Ricatti equation and thus can be linearized by the transformation

$$H_0(w) = -\frac{1}{b}\frac{K'(w)}{K(w)} \tag{7.8}$$

so long as $K(w)$ satisfies the *linear* equation

$$K'' + 8^3 wK = 0 \tag{7.9}$$

A further change of variable reduces this to Airy's equation. Thus, solving it gives

$$H_0(w) = -\frac{2}{17^2}(19 + 6\sqrt{2})\frac{\mathrm{Ai}'(-8w)}{\mathrm{Ai}(-8w)} \tag{7.10}$$

The other solution, $\mathrm{Bi}(-8w)$, of Airy's equation is omitted, as the arbitrary constant arising from the integration must vanish for this solution to asymptotically match the $\rho = 0$ solution. Returning to the original variables gives the asymptotic form of the generating function:

$$\frac{\hat{g}(x, \tau, \varepsilon)}{\tau} \sim \frac{2}{17}(5 - 2\sqrt{2}) + \frac{4}{17^2}(19 + 6\sqrt{2}) \times \left\{\frac{\varepsilon}{2\tau}\right\}^{1/3} \frac{\mathrm{Ai}'(\{\varepsilon/2\tau\}^{-2/3}\{1/2 - 2x^2/\tau^2\})}{\mathrm{Ai}(\{\varepsilon/2\tau\}^{-2/3}\{1/2 - 2x^2/\tau^2\})} \tag{7.11}$$

This result asymptotically matches (6.15) for $\rho \to 0$. This is easily seen by using the result $\mathrm{Ai}'(s)/\mathrm{Ai}(s) \sim -\sqrt{s}$ as $s \to \infty$. This shows that the above choice of p and q gives the correct set of dominant balance terms and the initial conditions in solving Airy's equation were correctly chosen. Comparing this with the tricritical scaling form (1.5) gives

$$\gamma_t = -\tfrac{1}{3}, \qquad \phi = \tfrac{2}{3} \tag{7.12}$$

ACKNOWLEDGMENTS

It is a pleasure to thank A. J. Guttmann for helpful discussions and a careful reading of the manuscript. The authors are grateful to the Australian Research Council for financial support.

REFERENCES

1. R. Brak and A. J. Guttmann, *J. Phys. A* **23**:4581 (1990).
2. R. Brak and A. J. Guttmann, *J. Phys. A* **23**:2319 (1990).
3. M. Bousquet-Mélou, Ph.D. thesis, University of Bordeaux.
4. K. Y. Lin, *J. Phys. A* **1**:1 (1992).
5. R. Brak, A. Guttmann, and S. Whittington, *J. Phys. A* **25**:2437 (1992).
6. A. L. Owczarek, T. Prellberg, and R. Brak, *J. Stat. Phys.* **72**:737–772 (1993).
7. D. B. Abraham and E. R. Smith, *J. Stat. Phys.* **43**:621 (1986).
8. A. L. Owczarek and T. Prellberg, *J. Stat. Phys.* **70**:1175–1194 (1993).
9. A. L. Owczarek, *J. Phys. A* **26**:L647–L653 (1993).
10. T. Prellberg and R. Brak, *J. Stat. Phys.*, submitted.
11. D. B. Abraham, *Phys. Rev. Lett.* **50**:291 (1983).
12. D. B. Abraham and P. J. Upton, *Phys. Rev. Lett.* **69**:225 (1992).
13. D. B. Abraham and P. J. Upton, *Phys. Rev. Lett.* **70**:1567 (1993).
14. H. N. V. Temperley, *Phys. Rev.* **103**:1 (1956).
15. M. E. Fisher, A. J. Guttmann, and S. Whittington, *J. Phys. A* **24**:3095 (1991).
16. R. Brak, A. L. Owczarek, and T. Prellberg, *J. Phys. A* **26**:4565–4579 (1993).
17. D. Polya, *J. Comb. Theor.* **6**:102 (1969).
18. D. Gouyou-Beauchamps, M. Delest, and B. Vauquelin, *Graphs Combinatorics* **3**:325–329 (1987).
19. M. P. Delest, *J. Comb. Theor. A* **48**:12–31 (1988).
20. M. Bousquet-Mélou, preprint, University of Bordeaux.
21. D. A. Klarner, *Fibonacci Q.* **3**:9–20 (1965).
22. V. Privman and G. Forgacs, *J. Phys. A* **20**:L543–547 (1987).
23. V. Privman and N. M. Švrakić, *Phys. Rev. Lett.* **60**:1107–1109 (1988).
24. D. B. Abraham and E. R. Smith, *Phys. Rev. B* **26**:1480 (1982).
25. H. T. Davis, *Introduction to Non-linear Differential and Integral Equations* (Dover, New York, 1962).
26. C. M. Bender and S. A. Orszag, *Advanced Mathematical Methods for Scientists and Engineers* (McGraw-Hill, Singapore, 1978).